VLSI Multi-Channel Track-and-Hold Potentiostat

Roman Genov[a], Milutin Stanacevic[b], Mihir Naware[c], Gert Cauwenberghs[b], Nitish Thakor[c]

[a] Department of Electrical and Computer Engineering,
University of Toronto, Toronto, ON M5S 3G4, Canada
[b] Department of Electrical and Computer Engineering,
Johns Hopkins University, Baltimore, MD 21218
[c] Department of Biomedical Engineering,
Johns Hopkins University School of Medicine, Baltimore, MD 21205

ABSTRACT

Simultaneous mapping of neural activity facilitates understanding neurological phenomena and their underlying mechanisms. We present a track-and-hold potentiostat performing simultaneous acquisition of 16 independent channels of current ranging five orders of magnitude in dynamic range over four scales down to hundreds of picoamperes. Sampling rate ranges from DC to 200KHz. The system features programmable current gain control, configurable anti-aliasing log-domain filter, triggered current integration and provides differential output ready for asynchronous external analog-to-digital conversion over a compressed dynamic range. We present system description, circuit implementation and experimental results of real-time neurotransmitter concentration measurements from the 16-channel prototype fabricated in a 1.2 μm CMOS process.

Keywords: Potentiostat, biomedical instrumentation, dopamine sensor arrays, analog VLSI, current-mode circuits, log-domain signal processing

1. INTRODUCTION

An emerging trend in neuroscience and neurophysiology is the movement towards understanding the fundamental behavior of neurons at the ensemble or population level by studying individual neurons at multiple sites. The electrophysiology of populations of neurons has been greatly aided by the development of multi-channel or array electrodes in integrated circuit technologies. Neurochemical elements exhibit considerable heterogeneity in their distributions and functions. Therefore, a technology that enables simultaneous monitoring of neurochemical activity at different locations in the brain promises to make fundamental discoveries in regional heterogeneity and specialization of neurochemistry of brain tissue.

Our group[1] has demonstrated microfabricated carbon-based sensor arrays for monitoring the concentration of electroactive neurotransmitters from distributed locations in the brain. Such techniques are based on the measurement of oxidation-reduction currents, associated with neurotransmitter activity, on sensor electrodes. Carbon electrodes can be manufactured using screen printing techniques for selective sensitivity to certain neurotransmitters. Such an instrumentation technology requires the interfacing of the distributed electrodes to a single-chip multi-channel VLSI potentiostat, essential to reduce the noise and system complexity inherent to having many individual cumbersome bench-top instruments with many connections. The integrated sensor-potentiostat system offers a very unique device for integrated neurochemical sensing and data acquisition. The primary neurotransmitters of interest are nitric oxide (NO) and dopamine. Both have multiple implications in numerous brain injury and disease phenomena.

Further author information:
E-mail: *roman@eecg.toronto.edu, miki@jhu.edu, mihir.naware@jhu.edu, gert@jhu.edu, nthakor@bme.jhu.edu*

1.1. Measurement of the electrical activity of neurons

Activity of neurons in the brain has classically been measured using microelectrodes: glass pipette electrodes are used for patch clamp or intracellular recording and metal microelectrodes are used for extracellular recordings.[2] From the timing pattern of the firing of the neuron, its role in information processing in the brain can be inferred. It is well accepted that information is encoded by the timing of individual neurons firing, however comprehensive information can only be gleaned by simultaneously recording the activity of multiple neurons.[3] Microfabrication techniques have been employed to construct arrays of microelectrodes on silicon substrates,[4, 5] or on glass culture plates.[6] Sophisticated semiconductor fabrication techniques have been employed to devise arrays of microsensors,[7] and, in some cases, analog interface circuitry.[8] Potentiostats with one or few parallel channels have been previously reported by our[11, 12] and other groups.[9, 10] The ability to record and analyze information from larger populations of neurons is of tremendous potential. For example, such recording from populations of neurons and interpreting their information coding could have far-reaching impact on understanding the neurophysiology of sensory-motor systems, encoding in auditory nerve and visual cortex.

1.2. Measurement of the chemical activity of neurons

The microelectrode and the microfabricated sensor technique described above are only suitable for measuring neurons electrical activity. This electrical activity is generated and modulated by the action of neurotransmitters. The neurotransmitters can be excitatory, such as glutamate, or inhibitory, such as GABA.[13] Other neurotransmitters such as dopamine, acetylcholine or serotonin are involved in a variety of physiological and pathophysiological functions.[14] Another type of neuronal messenger is nitric oxide (NO) which unlike the other chemical messengers, exists in a gaseous form.[15, 16] In contrast to other neurotransmitters that are chemically released at the synapses, NO is a retrograde messenger released from the post-synaptic cell and is capable of diffusing and influencing the presynaptic activity.

Much of the interest in the neurotransmitters stems from their importance in regulating the basic neuronal functions. However, abnormal levels of neurotransmitters can have pathophysiological consequences such as, for example, abnormal dopamine in Parkinsons disease and excess glutamate in excitotoxicity following ischemic brain injury. Neurotransmitters are localized in the brain by immunohistology, or measured by the microdialysis method. For continuous measurements, a microsensor based on carbon or platinum, coated with appropriate selective membrane can be used to detect the neurotransmitter levels.[17] The neurotransmitter action can then be detected using a potentiostat by voltammetry or amperommetry methods.[18] Sensing activities of neuronal messengers and relating them to the comcomitant neuronal electrical activity poses one of the most challenging problems.

1.3. The VLSI potentiostat chip and sensor interface

Continuous measurement of neurotransmitters in brain tissue is now possible using electrochemical sensor technology. Integrated microsensor arrays described above[1] are capable of mapping the spatial and temporal distribution of neuronal messengers or neurotransmitters such as nitric oxide (NO) and dopamine. The wiring connecting all the sensors can be extensive and noise problems typically arise. Additionally, an array of external commercial bench-top potentiostat instruments, can be prohibitively expensive. Therefore, we have designed and fabricated a single-chip VLSI system, which allows to perform data acquisition in the close proximity of the sensor array.

To simultaneously transduce the neurotransmitter activity at multiple locations in brain tissue in close proximity to a neurochemical sensor array, a multi-channel potentiostat amplifier has been developed. The integrated system simultaneously acquires the oxidation-reduction currents generated at the surface of each element of the sensor array, amplifies them and converts them to voltages. These voltages are proportional to the neurotransmitter concentration. Each potentiostat channel is interfaced with one working electrode, maintained at virtual ground, with a redox potential applied to the reference electrode. The potentiostat provides the necessary voltage for driving the redox reactions at the sensor with respect to a reference in the bath and a counter electrode on the electrode array.[19] The electrochemical current output from the electrode is usually on the order of picoamperes, but can reach the microampere range during transients or catastrophic events such as stroke.[20]

The track-and-hold potentiostat system presented here integrates 16 current-mode inputs, 4 voltage references setting the voltage levels of the virtual-ground current inputs in groups of 4, and a single full-range differential

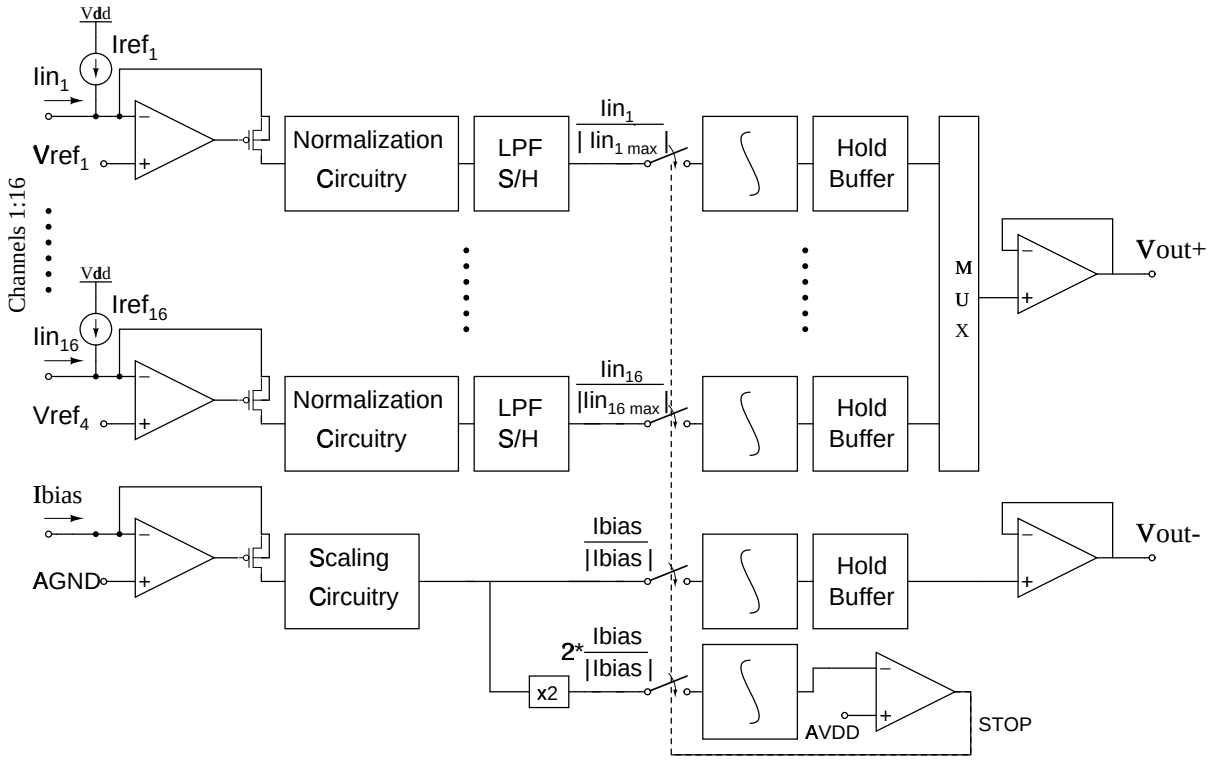

Figure 1. *Block diagram of the integrated track-and-hold potentiostat.*

voltage output. Each of the 16 channels is independently configured for a gain of attenuation covering four orders of magnitude allowing to acquire bidirectional currents in the range from 100 pA to 50 μA, at a reference voltage ranging from 0 to 5V. Programmable cut-off frequencies ranging from 50Hz to 400kHz prevent aliasing of high frequency components and allow to decrease the level of noise generated prior to sampling. The maximum fully sustained sampling rate ranges from DC to 200KHz. The outputs of the system are pipelined and continuously valid, interfacing asynchronously to an external ADC on the PC host acquisition board for data post-processing. Thus, the integrated potentiostat interfaces between a sensor array and a remote PC acquisition system, for fast simultaneous synchronous current sensing over a wide dynamic range down to hundreds of picoamperes.

2. ARCHITECTURE

The block diagram of the single-chip track-and-hold potentiostat system is presented in Figure 1. There are 16 data channels that are controlled by the bias channel (bottom of Figure 1) which also supplies all bias and reference signals. An input signal to each data channel is summed with an appropriately scaled reference current I_{ref} to obtain a unidirectional input signal. This scaled reference current is digitally selected as one of the currents generated in the bias channel. The input to the bias channel is a 50 μA DC current. A transconductance amplifier drives a PMOS load transistor to provide a high input conductance input stage. The acquired input current is then fed into a scaling circuit which is programmed to normalize the signal to a fixed range over the interval [0, 1] μA. This range is chosen appropriately as a trade-off between signal-to-noise ratio and integration time constant further in the channel. The normalized current is fed into an anti-aliasing low-pass filter. Besides serving for anti-aliasing, the cut-off frequency of the filter can be programmed to match the integration time interval when the sample-and-hold is operated in the transparent mode.

The integrator at the end of the channel is used for current-to-voltage acquisition. Integration of 0.5 μA and 1 μA reference currents in the bias channel determine the conversion gain of all 16 channels. This is achieved by controlling the upper-bound voltage and the midpoint voltage of conversion, as set by an externally supplied

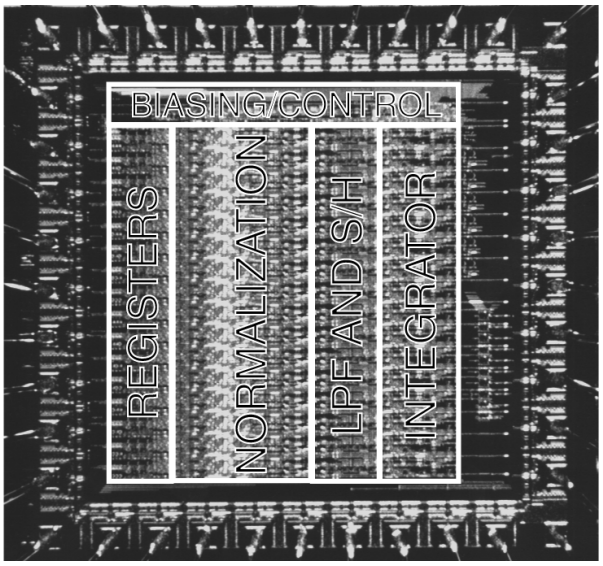

Figure 2. *Chip micrograph of the 16-channel integrated track-and-hold potentiostat. Die size is* 2.25×2.25 mm^2 *in 1.2* μm *CMOS technology.*

reference. Once the integrated voltage of the upper-bound reference channel goes above the analog V_{ref} level, a trigger signal (STOP) is generated which completes integration in all channels (including the bias channels themselves). A 16-to-1 multiplexer selects the integrated signal of one of the 16 channels at the output. The midpoint voltage generated by the second reference channel is used as a 'zero-level' reference of the output signal, serving a differential output format for reduced sensitivity to noise and power supply variations. In hold mode, the differential output from the previous integration cycle is buffered and held at the output while the current integration process is taking place.

3. VLSI IMPLEMENTATION

The integrated track-and-hold potentiostat was designed and fabricated in a 1.2 μm double-poly CMOS process, which includes a p-Base layer to implement vertical NPN bipolars. The chip micrograph is shown in Figure 2. The sections below focus on particular circuit design solutions and their experimentally observed performance.

3.1. Input Transconductance Amplifier

For precision acquisition of small currents, a transconductance amplifier was used, depicted in Figure 3, to provide a high input conductance virtual 'ground' at a user-selectable reference voltage. It constitutes a wide output range single stage differential amplifier with a PMOS differential pair and cascoded BiCMOS current mirrors. The differential pair transistors were laid out in a centroid configuration to lower input voltage offset. Higher accuracy current replication is obtained by using current mirrors base current compensation with MOS voltage followers. The choice of 7V for Vdd level and -2V for Vss level allows the reference voltage to range from 0V to 5V (a typical range of GND and V_{dd} for multi-electrode carbon sensors).

A PMOS load at the input, in the feedback loop of the amplifier, conveys the current at the supplied reference voltage as shown in Figure 1.[21] The PMOS transistor has the well connected to the source to minimize the back-gate effect, as needed for a 5V range of the input reference voltage. Figure 4 depicts measured DC input voltage offsets for all channels for a range of input reference voltages at a fixed current, and for a range of input currents at a fixed input reference voltage. Taking into account the measured mismatch, the DC input offsets are in the range between 5mV and 10mV (for single ended input), for the minimum and maximum input current scales respectively, with the input impedance of 125Ω. These offset figures are typical for the process used even for a centroid configuration, and higher precision, if so required, can be obtained by using a more advanced (and more expensive) fabrication process.

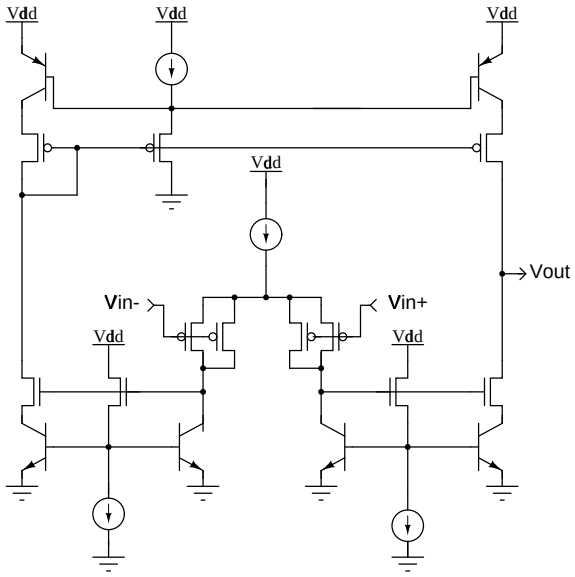

Figure 3. *Input transconductance amplifier with a differential pair in centroid layout configuration.*

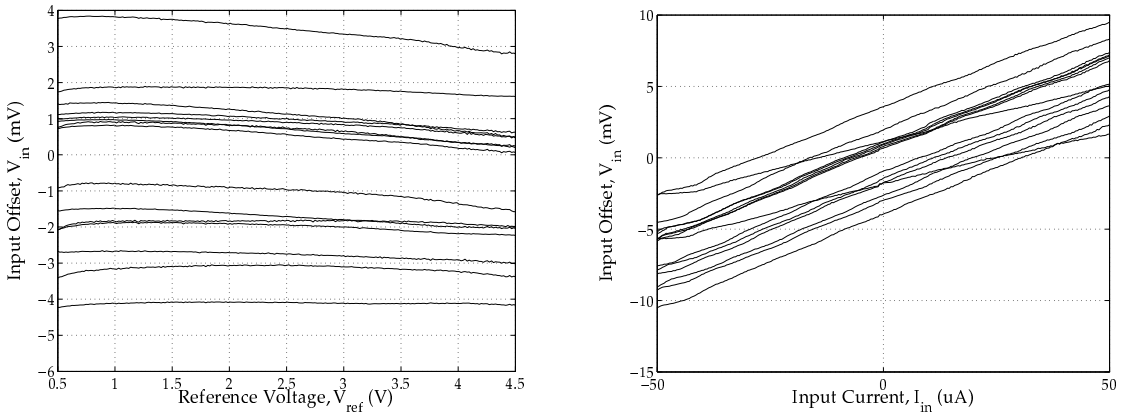

(a) *(b)*

Figure 4. *Measured input voltage offsets of input transconductance amplifiers for 16 channels: (a), for the a range of input reference voltages at zero input current; (b), for a range of input currents at 2.5V input reference voltage.*

3.2. Current Normalization

The acquired input current of each of the data channels is normalized to a fixed range suitable for further processing. Normalization circuitry shown in Figure 5 performs this task. The programmable scaling selects between four input ranges of current, 100 nA, 1 μA, 10 μA, 100 μA, independently for every data channel. This scaling function provides for a floating point representation, and drastically increased dynamic range. The four BiCMOS current mirrors can be configured to attenuate the input signal with a gain of 0.01, 0.1, 1 or 10 by means of switching of bipolar transistors bases. Vertical NPN and lateral PNP transistors were used in the design. Amplification of currents with gains other than one is performed using NPN vertical transistors, as the gain control by scaling of the emitter area is more precise and reproducible. The output current is a replica of the input current normalized to a range 0–1 μA. Any nonlinear effects in the normalization, and in subsequent processing stages, can easily be accounted for by a look-up table type calibration in software. The main concern in the design is signal-to-noise performance.

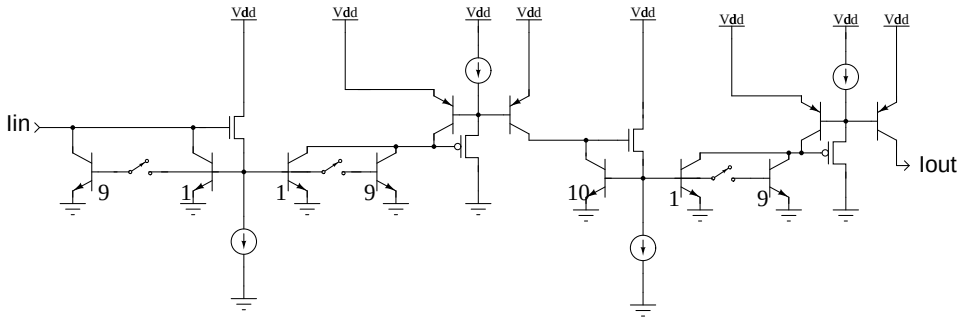

Figure 5. *Data channel current normalization circuitry. Normalization is performed over four orders of magnitude of the input current. The lowest input current scale is 0–100 nA, the highest is 0–100 μA.*

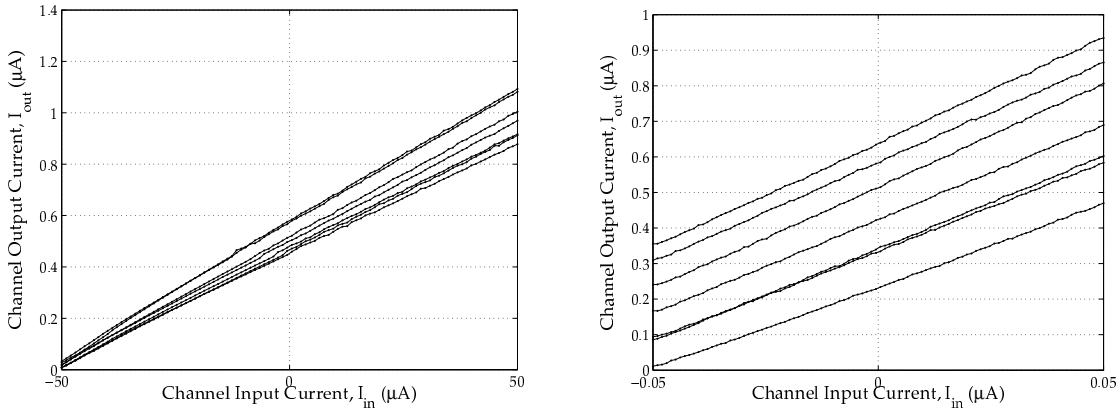

Figure 6. *Measured channel output current for multiple adjacent channels: (a) at the largest (100 μA) input current scale and (b) at the smallest (100 nA) input current scale.*

3.3. Low-Pass Filter

To allow aliasing-free sampling of the normalized currents, a low-pass filter with selectable cut-off frequency is incorporated into the channel. A two stage log-domain LPF was designed as shown in Figure 7.[22–24] It is composed of two basic first-order log-domain circuits, which use translinear circuits as their building blocks. A basic one-stage log-domain filter exhibits a global linear transfer function while internally consisting of non-linear exponential components. Each stage constitutes a single pole LTI system with unity DC gain if the bias currents are supplied as shown in Figure 7. As it can be observed from the circuit diagram, two single-stage log-domain filters are combined in such a way that the output common-base configuration NPN transistors of the first stage serve as the input transistor pair of the second stage.[24] The resulting two-stage filter has better defined pass-band corners. The cut-off frequency set by the current I_{bias} can be programmed and selectable in the range from 50Hz to 400kHz.

The filter prevents aliasing and eliminates high-frequency noise and interference introduced prior to sampling, and additionally allows to bypass the subsequent current-mode sample-and-hold circuit before the integration stage, by selecting a time constant sufficiently larger than the integration time interval. The experimental noise measurements of the output filter current showed an input-referred RMS noise value of 46pA (for a measured attenuation factor of 13) at a 12kHz bandwidth. This indeed allows to resolve input currents as low as 100pA and establishes the dynamic range of the system well in excess of 100dB. Figure 6 depicts measured channel current transfer characteristics for for the largest and the smallest current scale for multiple adjacent channels. Channel-wise calibration is performed to remove mismatch-induced current and gain errors, as well as higher order errors.

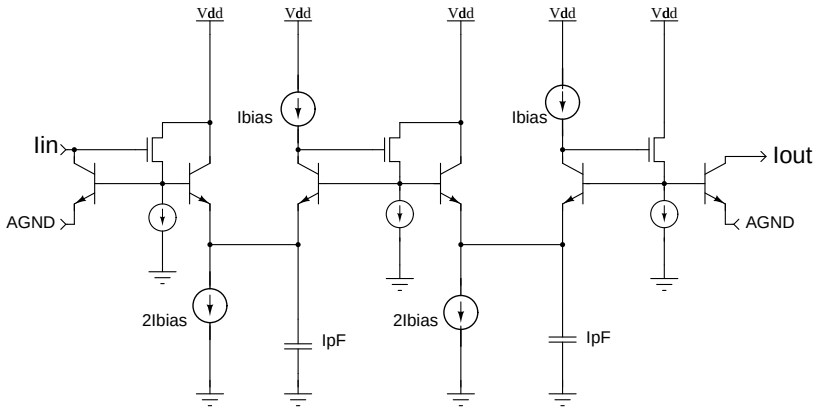

Figure 7. *Anti-aliasing two-stage log-domain LPF.*

A current-mode sample-and-hold circuit, not shown, follows the anti-alias filter stage. Its operation is synchronized with the subsequent integration stage, and can be disabled (*i.e.,* made transparent) in software. The sample-and-hold can be used for high-speed acquisition at speeds exceeding the integration time interval of the integrator (5 μs), although signal-to-noise considerations (high frequency sampling noise) dictate this feature to be used only in the largest (50 μA) current scale.

3.4. Integration and Hold Buffer Circuitry

Integration circuitry described in this section performs conversion of normalized currents into differential voltage and produces a continuously available output signal. The system level operation principle of the integrators is described in detail in Section 2. As described earlier, an integration circuit is employed once in every data channel, and separately in two reference channels, one to control the conversion gain factor, and the other to provide a zero-level reference for the converted output voltage signal.

The circuit diagram of one integrator channel is given in Figure 8. Transistors N1, N2 and P1 and a PMOS current source realize an inverting transconductance amplifier. The mirrored input current is integrated on a 1pF capacitor across the amplifier. The digital signal TRIG is a narrow pulse resetting the integrating capacitor on the rising edge, and also resetting the STOP signal (described in Section 2) on the falling edge. The digital signal $\overline{\text{H}}$ is a delayed version of TRIG. Once TRIG switches high, the integrating capacitor is reset. When TRIG turns low, the input current is activated, and is integrated on the capacitor. Duration of the integration process is determined by the width of the STOP pulse, which itself is determined by the time the integration takes to attain the nominal value, by the procedure explained above. This corresponds to a 5 μs integration time, or 200KHz maximum sustained sampling frequency. Higher conversion rates are achievable by activating the sample-and-hold cell included in the preceding stage. Figure 9 illustrates example waveforms of the signals described above for zero integrator input current and normalization range [0, 4] μA.

In order to produce continuously available output voltage, during the previous integration cycle, the output voltage is sampled on a 0.5pF capacitor and held while a new current is integrated in pipelined fashion. The control of this feature is carried out in software by the digital signal THRU. Figure 10 depicts measured channel transfer characteristics (integrator output voltage) for multiple adjacent channels at the largest current scale. Channel-wise calibration is performed to remove mismatch-induced current, gain, and higher order errors.

The measured characteristics of the integrated track-and-hold potentiostat system are summarized in Table 1.

4. REAL-TIME MEASUREMENT OF NEUROTRANSMITTER CONCENTRATION

The 16-channel single-chip potentiostat has been experimentally demonstrated to facilitate real-time measurements of neurotransmitter concentration. The integrated system was interfaced with carbon micro-fiber electrodes to monitor temporal variations in dopamine concentration in a solution.

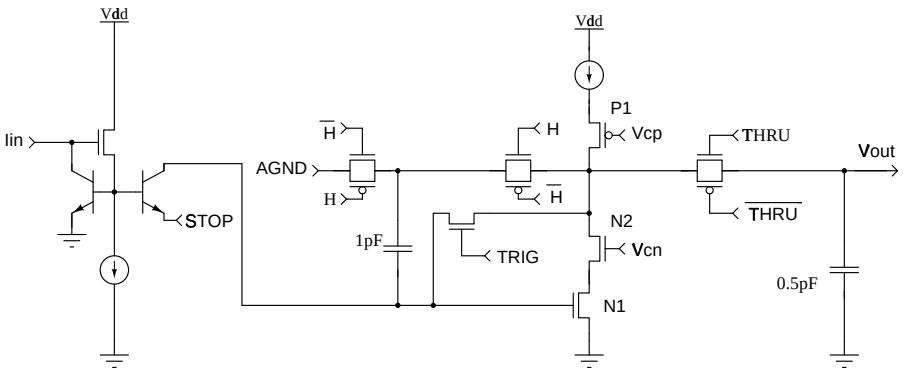

Figure 8. *Integration and track-and-hold circuitry.*

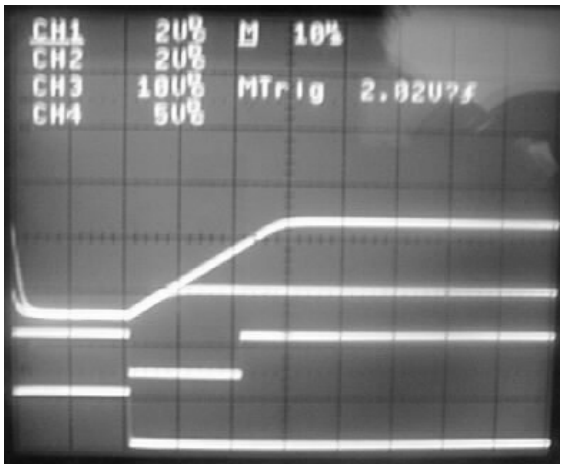

Figure 9. *Integrator control signals and example observed output voltages waveforms. From top to bottom:* V_{out-}, V_{out+}, *STOP, and TRIG.*

A standard solution of dopamine was prepared by dissolving 20mg of dopamine hydrochloride in 99 *ml* of degassed, deionized water. 1 *ml* of perchloric acid was added to keep the solution stable over time. Commercially available carbon micro-fiber electrodes were utilized. The OD of the carbon micro-fiber was 30 μm. The sensors were also coated with nafion, which is a cationic exchange resin. Its charge selective properties prevent the diffusion of negatively charged ionic species across it, thus preventing such species from reaching the surface of the carbon electrode. Its presence does not interfere with the oxidation of dopamine, however. Prior to interfacing with the 16-channel VLSI potentiostat, the carbon fiber electrodes were tested using a commercial bench-top potentiostat/galvanostat controlled by a microcomputer via a GPIB interface. The electrodes were electrochemically activated by successive cycling from 0 V up to +3.0 V for 20 s, +2.4 V for 15 sec and +1.8 V for 10 sec at 70 Hz.[20] This pre-treatment increases the sensitivity and stability of the response of the electrodes through the production of an oxide layer and a net increase of surface area.

A two-electrode system was employed, in contrast with the more traditional three-electrode configuration. This is because the current produced by the oxidation of neurotransmitter species at physiological concentrations is typically in the nano/pico ampere level, and as such, it is expected that these current levels do not affect the reference electrode. Each test was conducted in 25 *ml* of degassed phosphate-buffered saline solution (PBS w/o Mg++ and Ca++) at a pH of 7.4. Controlled amounts of dopamine solution were introduced from gas-tight syringes directly into the solution following which the solution was briefly stirred to ensure uniform dissolution of the analyte. The current was allowed to stabilize for four minutes before the next bolus of dopamine was added. Standard chronoamperometry was employed to measure the current, in which the working carbon electrode was held at 900mV with respect to the Ag/AgCl reference electrode. The current was recorded as a function of time

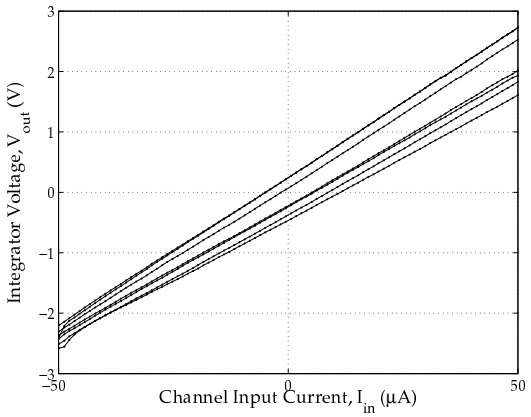

Figure 10. *Measured integrator output voltage for multiple adjacent channels at the largest current scale (100 μA).*

Table 1. Measured Chip Characteristics

Channels	16			
Max Sampling Rate	200KHz			
Input Current Range	-50nA- +50nA	-500nA- +500nA	-5μA– +5μA	-50μA– 50μA
Input-Referred RMS Current Noise	46pA	1nA	8nA	25nA
Input Impedance	125Ω			
DC Offset	+/-5mV	+/-5mV	+/-5mV	+/-10mV
Power Dissipation	12.5mW			
Analog Volt. Range	0-5V			
LPF Cut-off Freq.	50Hz - 400KHz			
Power Suppl. Volt.	-2V; +7V			
Technology	1.2μm, BiCMOS (vertical NPN), double poly			
Die Size	2.25 mm x 2.25 mm			

as shown in Figure 11. The calibration curve of the sensor-chip system depicted in Figure 12 was obtained by calculating average currents for discrete concentration levels.

5. CONCLUSIONS

A 16-channel integrated potentiostat for simultaneous parallel recording of neurochemical activity has been presented. It has been tested to operate with a dynamic range of 100dB and allows to resolve analog currents as low as 100pA. The system features programmable current gain control, configurable anti-aliasing circuitry, triggered current integration and provides differential output ready for asynchronous external A/D conversion over a compressed dynamic range. With a sampling rate ranging from DC to 200KHz and dynamic range covering five orders of magnitude, the potentiostat integrated system has been demonstrated to facilitate real-time measurements of neurotransmitter concentration.

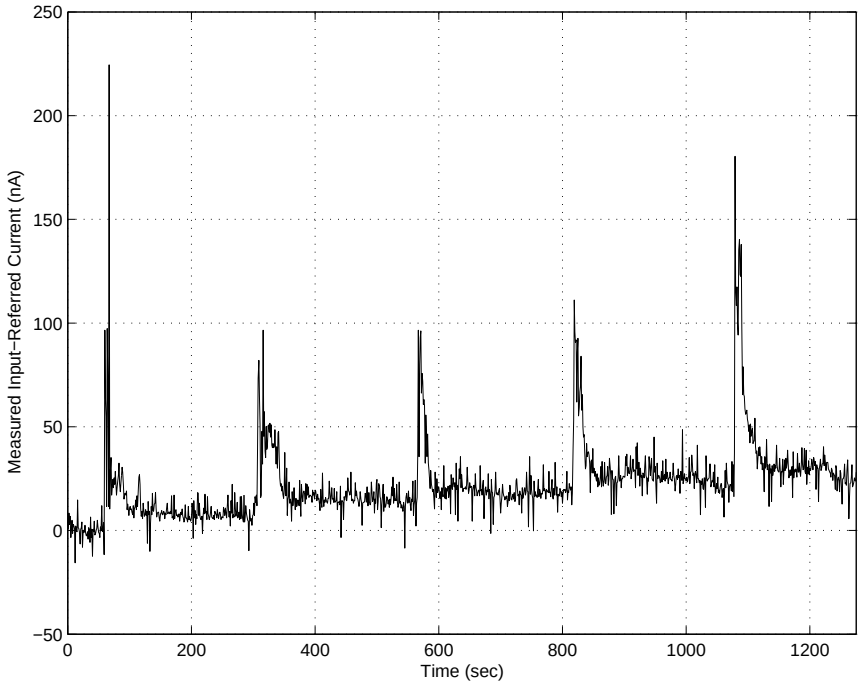

Figure 11. *Measured input-referred chronoamperometry sensors output current. Controlled amounts of dopamine solution were introduced into degassed phosphate-buffered saline solution every four minutes and briefly stirred.*

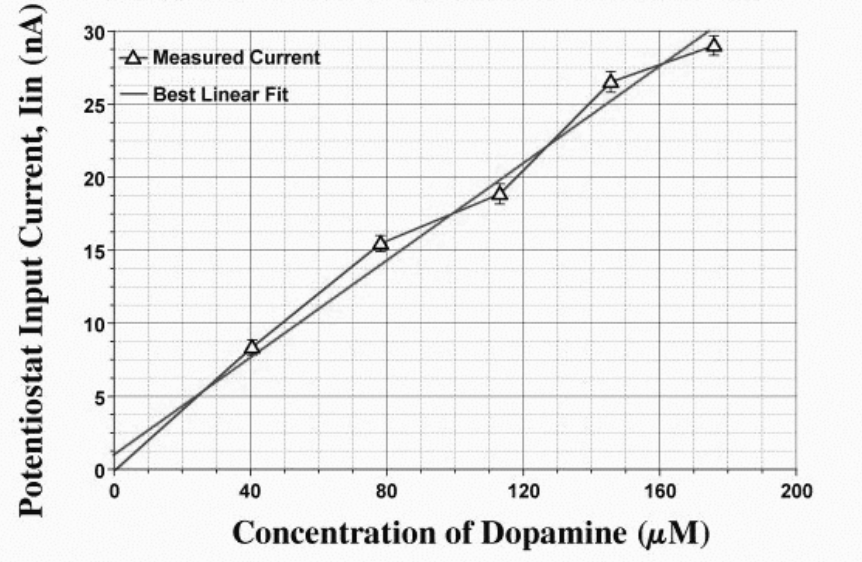

Figure 12. *Sensor calibration plot: time-averaged carbon electrode output current as a function of the concentration of the analyte dopamine in a solution. The best linear fit is also shown. The molar weight of dopamine is 189.64 gm/mol.*

ACKNOWLEDGMENTS

This work was supported in part by NSF under Career Award MIP-9702346, ONR YIP/PECASE N00014-99-1-0612, and Whitaker Foundation.

REFERENCES

1. P.M. George, J. Muthuswamy, J. Currie, N.V. Thakor, and M. Paranjape, "Fabrication of screen-printed carbon electrodes for sensing neuronal messengers," *BioMEMS,* vol. **3** (4): 307-313, December 2001.
2. R. Lemon, A. Prochazka, "Methods for Neuronal Recording in Conscious Animals," Wiley, John & Sons, Feb. 1984.
3. E. Maynard, C. Nordhausen, R. A. Normann, "The Utah Intracortical Electrode Array: a recording structure for potential brain-computer interfaces," *Electroencephalography and Clinical Neurophysiology,* vol **102** (3), pp 228-239, March 1997.
4. K.L. Drake, K.D. Wise, J. Farraye, D.J. Anderson, S.L. BeMent, "Performance of planar multisite microprobes in recording extracellular single-unit intracortical activity," *Biomedical Engineering, IEEE Transactions on,*, vol. **35** (9), pp. 719-732, September 1988.
5. N.A. Blum, B.G. Carkhuff, H.K. Charles Jr.; R.L. Edwards, R.A. Meyer, "Multisite microprobes for neural recordings," *Biomedical Engineering, IEEE Transactions on,* vol. **38** (1), pp 68-74, Jan. 1991.
6. Pine, J., "Recording action potentials from cultured neurons with extracellular microcircuit electrodes," *Journal of Neuroscience Methods,* vol.**2**, pp. 19-31, 1980.
7. Kovacs, G. T. A., Peterson, K., and Albin, M., "Silicon micromachining," *Analytical Chem.* vol. 68, pp. 407A-412A, 1996.
8. Ji J. and Wise, K. D., "An implantable CMOS circuit interface for multiplexed microelectrode recording array," *IEEE J. Solid State Circuits,* vol. **27**, pp 433-443, 1992.
9. R.B.F. Turner, D.J. Harrison, and H.P. Baltes, "A CMOS Potentiostat for Amperometric Chemical Sensors," *IEEE J. Solid-State Circuits,* vol. **SC-22**, pp. 473-478, 1987.
10. R.G. Kakerow, H. Kappert, E. Spiegel, and Y. Manoli, "Low Power Single Chip CMOS Potentiostat," *Transducers 95, Eurosensors IX*, vol. **1**, pp. 142-145, 1995.
11. A. Bandyopadhyay, G. Mulliken, G. Cauwenberghs, and N. Thakor, "VLSI Potentiostat Array for Distributed Electrochemical Neural Recording," *Proc. IEEE Int. Symp. Circuits and Systems (ISCAS'2002),* Phoenix AZ, May 26-29, 2002.
12. G. Mulliken, M. Naware, A. Bandyopadhyay, G. Cauwenberghs and N. Thakor, "Distributed Neurochemical Sensing: *In Vitro* Experiments," *Proc. IEEE Int. Symp. Circuits and Systems (ISCAS'2003),* Bangkok Thailand, May 25-28, 2003.
13. Purves, D., Augustine, G. J., Fitzpatrick, D., Katz, L. C., LaMantia A., McNamara, J. O, "Neuroscience," ed. Sunderland, MA: Sinauer Associates, Inc., 1997.
14. Siegel, G. J., Agranoff, B. W., Albers, R. W., and Molinoff, P. B., "Basic Neurochemistry," New York, N.Y.: Raven Press, 1993.
15. Snyder, S.H. "Nitric Oxide: First in a new class of neurotransmitters?" *Science*, vol. **257**, 1992.
16. Vincent, S. "Nitric Oxide in the Nervous System," *Neuroscience Perspectives*, P. Jenner, Ed., San Diego, CA, Acad. Press, pp. 317, 1995.
17. Paula S. Cahill, Q. David Walker, Jennifer M. Finnegan, George E. Mickelson, Eric R. Travis, and R. Mark Wightman, "Microelectrodes for the Measurement of Catecholamines in Biological Systems," *Anal. Chem.*, vol. **68** (18), pp 3180 - 3186, 1996.
18. Coury, L. A. Jr., Huber, E. W., and Heinman, W. R., "Application of modified electrodes in the voltammetric determination of catecholamine neurotransmitters," *Applied Biosensors*, Butterworths, Boston, 1989.
19. J.C. Hoogvliet, J.M. Reijn, V. Bennekom, and P. Wouter, "Multichannel Amperometric Detection System for Liquid Chromatography and Flow Injection Analysis," *Analytical Chemistry,* vol. **63**, pp. 2418-2423, 1991.
20. J.-K. Park, P.H. Tran, J.K.T. Chao, R. Godhadra, and N.V. Thakor, "In Vivo Nitric Oxide Sensor Using Non-Conducting Polymer Modified Carbon Fiber," *Biosensors Bioelectronics,* vol **13**, pp 1187-1195, 1998.
21. Sedra, A.S. and Roberts, G.W., "Current Conveyor theory and practice." In C. Toumazou, F.J. Lidgey and D.G. Haigh (Eds.), *Analogue IC design: The current mode approach,* 1990, pp. 93-126.
22. Y. Tsividis, "Externally Linear, Time-Invariant Systems and Their Applications to Companding Signal Processors," *IEEE T. Circuits and Systems II,* vol. **44** (2), pp. 65-85, 1997.

23. D. Frey, "Log-Domain Filtering for RF Applications," *IEEE J. Solid-State Circuits,* vol. **31** (10), pp. 1468-1475, 1996.

24. R. Edwards, G. Cauwenberghs, "A Second-Order Log-Domain Bandpass Filter for Audio Frequency Applications," Proc. IEEE Int. Symp. on Circuits and Systems (ISCAS'98), Monterey, CA, June, 1998.

25. E. Vittoz and J. Fellrath, "CMOS Analog Integrated Circuits Based on Weak Inversion Operation," *IEEE Journal on Solid-State Circuits,* vol. **12** (3), pp 224-231, 1977.

26. A.G. Andreou, K.A. Boahen, P.O. Pouliquen, A. Pavasovic, R.E. Jenkins, and K. Strohbehn, "Current-Mode Subthreshold MOS Circuits for Analog VLSI Neural Systems," *IEEE Transactions on Neural Networks,* vol. **2** (2), pp 205-213, 1991.

27. E. Vittoz, "Low-Power Design: Ways to Approach the Limits," *1994 IEEE ISSCC Proceedings,* vol. **37**, pp 14-18, 1994.

28. C. Mead, *Analog VLSI and Neural Systems*, Addison-Wesley, 1989.

29. M. Ismail and T. Fiez, Eds., *Analog VLSI for Signal and Information Processing*, McGraw-Hill, 1995.

30. E. Vittoz, "Micropower Techniques," in *Design of Analog-Digital VLSI Circuits for Telecommunications and Signal Processing*, Franca and Tsividis, Eds., Prentice Hall, 2nd. ed., pp 53-96, 1994.